Article

Ni-Decorated ZnO Monolayer for Sensing CO and HCHO in Dry-Type Transformers: A First-Principles Theory

Jin Zhang *, Yuqing Wang, Zhuo Wei, Qi Wang, Zhengbo Liang and Tian Yuan

China Electric Power Research Institute, Wuhan 430074, China; wangyuqing@epri.sgcc.com.cn (Y.W.);
weizhuo@epri.sgcc.com.cn (Z.W.); wangqi5@epri.sgcc.com.cn (Q.W.); liangzhengbo@epri.sgcc.com.cn (Z.L.);
yuantian3@epri.sgcc.com.cn (T.Y.)
* Correspondence: zhangjin@epri.sgcc.com.cn

Abstract: This work implements first-principles simulations in order to investigate the Ni-decorating property on the ZnO monolayer and the sensing property of the Ni-decorated ZnO (Ni–ZnO) monolayer upon CO and HCHO molecules formed in the dry-type transformers. The results reveal that the Ni dopant is stably anchored on the T_O site of the ZnO surface forming the Ni–Zn and Ni–O bonds with the binding energy (E_b) of -1.75 eV. Based on the adsorption energy (E_{ad}) of -1.49 and -2.22 eV for CO and HCHO on the Ni–ZnO monolayer, we determined the chemisorption for two such systems. The band structure (BS) and atomic density of state (DOS) of the gas adsorbed systems are analyzed to comprehend the electronic property of the Ni–ZnO monolayer in the gas adsorptions. Besides, the change of bandgap and work function uncover the sensing potential of Ni–ZnO monolayer upon CO and HCHO detections, with admirable electrical response (15,394.9% and -84.6%). The findings in this work manifest the potential of Ni–ZnO monolayer for CO and HCHO sensing to evaluate the operation condition of the dry-type transformers.

Keywords: Ni–ZnO monolayer; dry-type transformers; sensing property; first-principles theory

1. Introduction

Dry-type transformers are widely applied in electrical systems to transmit and transform electricity [1]. In these systems, the epoxy resin, as the insulating medium, plays a significant role in keeping the safe operation of such equipment from some insulation defects, including partial overheat and discharge [2]. To promote the performance of the epoxy resin, some chemical addition, such as epoxy chloropropane (ECH), would be added to increase the burning point so as to avoid certain burning accident of the dry-type transformers [3]. Even though inevitable defects, especially partial overheating, such inner transformers would decompose the epoxy resin into several gas compounds [4]. As reported, the dominant gas species of the epoxy resin are CO and HCHO [5], which would be diffused around the transformer substation and pose a great challenge for maintenance workers. Besides, the formation of these gas species indicate the deteriorated quality as well as the weakened insulation performance of the epoxy resin, which would threaten the good operation of the dry-type transformers [6]. Considering this, CO and HCHO are regarded as the typical gases to reflect the operation status of the transformers and performing their detections is an effective approach to monitor the operation condition of the whole power system and the personal safety of the maintenance workers [7].

Gas sensing using the nanomaterials, especially the 2D buddies, has become very eye-catching in recent years, and pronounced attention has been for their applications in many fields [8–10]. Specifically, the past few years have witnessed great success in graphene-based materials for gas detections [11–13]. In the meantime, scholars are making every effort to explore graphene-like materials with similar or even more excellent properties for gas sensing use [14]. Recently, a ZnO monolayer with a 2D one-atom-layered structured by periodic Zn–O hexatomic rings was discovered. It was demonstrated to have admirable

electronic properties and good chemical stability [15]. Also, there have several reports about transition metals (TM) decorated ZnO monolayer for toxic gas detections [16–18]. In this regard, one can assume that the TM-decorated ZnO monolayer would be a promising material for sensing CO and HCHO in the dry-type transformers to evaluate its operation conditions accordingly.

In this paper, we selected the Ni metal as the representative dopant to decorate the pristine ZnO surface and to study the sensing performance of Ni-decorated ZnO (Ni–ZnO) monolayer upon two toxic gases, namely CO and HCHO, based on the first-principles theory. As reported, the Ni dopant can largely enhance the adsorption performance of the 2D nanomaterials therefore promote the sensing response of the whole system [19,20] due to its desirable catalytic behavior in the gas interactions. Also, there have been several reports concerning the admirable structural and electronic properties of Ni-decorated ZnO [21,22]. In this aspect, it is hopeful that the Ni–ZnO monolayer can conduct satisfied adsorption and sensing behaviors in the gas systems given its favorable sensing property upon C_2H_2 in the previous experimental report [23]. Therefore, we provided first-principles calculations to further investigate the sensing mechanism of the Ni–ZnO monolayer upon gas species, which to some extent can give guidance for exploring novel sensing materials from an experimental point of view as well. This work aims to explore the potential of the Ni–ZnO monolayer as a remarkable gas sensor to evaluate the working status of the dry-type transformers via faults gas detections, which is beneficial for guaranteeing the good operation of the power system.

2. Computational Details

All of the first-principles simulations are with spin-unrestricted set within the DMol^3 package [24], in which we selected the Perdew-Burke-Ernzerhof (PBE) function and the generalized gradient approximation (GGA) to treat the exchange correlation interaction [25]. The Van der Waals force and long-range interactions were treated by the DFT-D2 method with corrected dispersion [26]. The Monkhorst-Pack k-point mesh of $10 \times 10 \times 1$ was adopted for the Brillouin zone integration [27]. We defined the energy tolerance accuracy, self-consistent loop energy, and global orbital cut-off radius to be 10^{-5} Ha, 10^{-6} Ha and 5.0 Å [28], respectively. A $4 \times 4 \times 1$ ZnO supercell, with 16 Zn atoms and 16 O atoms, was configured to model the pristine ZnO monolayer, and a vacuum region of 20 Å was determined to avoid the adjacent units' interactions [29]. Moreover, the Hirshfeld method was used to consider the charge-transfer value (Q_T) of the gas species in adsorptions as well as the atomic charge of Ni dopant in the Ni–ZnO system.

3. Results and Discussion

3.1. Analysis of Ni–ZnO Monolayer

To investigate the Ni-decorating behavior on the intrinsic ZnO surface, we select several possible decorating sites, including T_O (on the top of O atom), T_{Zn} (on the top of the Zn atom), $B_{Zn–O}$ (on the bridge site of Zn–O bond), and $H_{Zn–O}$ (on the top of the hollow site of Zn–O ring). In the meantime, the binding energy (E_b) is introduced to reflect the binding force between the Ni dopant and the ZnO monolayer, calculated by:

$$E_b = E_{Ni-ZnO} - E_{ZnO} - E_{Ni} \tag{1}$$

wherein E_{Ni-ZnO}, E_{ZnO} and E_{Ni} indicate the energies of the Ni–ZnO monolayer, isolated ZnO monolayer and Ni atom, respectively. By Equation (1), the final decorating site, with the most negative E_b, is determined. The Ni-decorating process is plotted in Figure 1, in which the charge density difference (CDD) of the determined Ni–ZnO structure and the other possible configurations for Ni–ZnO monolayer are plotted as well. Also, we study the Ni-embedded behavior within the ZnO monolayer by replacing a Zn atom by the Ni atom for better comparison, which with related analyses can be found in the Supplementary File Figure S1. Through such comparison, we finally determine the Ni-decorating in the following calculations.
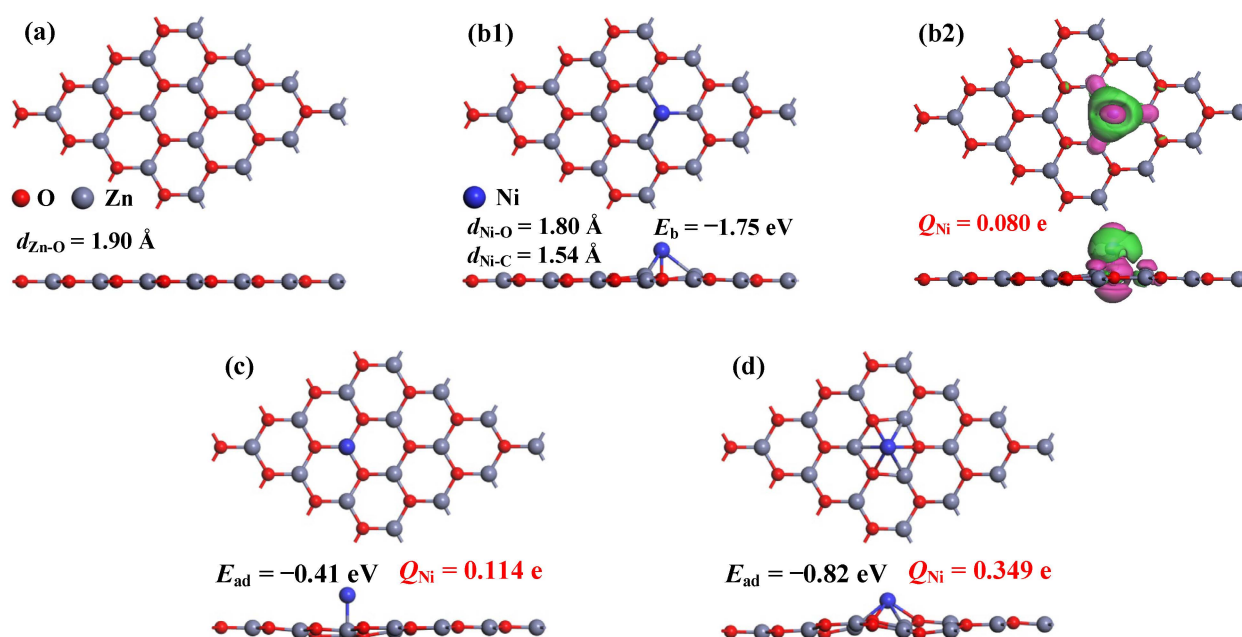
Figure 1. Ni-decorating behavior on the ZnO monolayer (**a**) pristine ZnO monolayer, (**b1,b2**) determined structure and related CDD of Ni–ZnO monolayer, (**c,d**) other possible configurations f Ni–ZnO monolayer. In CDD, In CDD, the green areas are electron accumulation while the violet areas are electron depletion with the isosurface of 0.01 eV/Å^3.

In the pristine ZnO system, the Zn–O bond is obtained as 1.90 Å and the constant lattice is 3.30 Å, which are in agreement with the previous report [30]. For Ni-decorating process, it is interesting to note that after geometric optimization, the Ni dopant at the B_{Zn-O} site suffers somewhat displacement and moves to the T_O site eventually, and the T_O site according to our calculations is regarded as the most preferred one for Ni-decorating on the pristine ZnO surface. On the T_O site, the Ni dopant is bonded with the underlying O atom and three neighboring Zn atoms, and the Ni–O and Ni–Zn bonds are obtained as 1.80 and 1.54 Å, respectively. Besides, the E_b for this site is calculated to be −1.75 eV, much more negative than those on the other sites (−0.41 eV for the T_{Zn} site and −0.82 eV for the H_{Zn-O} site which suggests that the good spontaneity and chemical stability for Ni-decorating on the ZnO surface at the top of the O atom [31]. Moreover, the vibrational analysis further verifies the chemical stability of the Ni–ZnO monolayer, by which the frequencies are ranging at 47.97~1353.83 cm^{-1}, without the imaginary frequency [32]. Also, the Ni dopant is positively charged by 0.080 e, suggesting its electron-donating property when decorating on the ZnO surface that may ascribe to its weaker electronegativity than the O atom [33]. From the CDD, there are strong electron depletion on the Ni dopant and electron accumulation on the Ni–O and Ni–Zn bonds, which not only supports the electron-releasing property of the Ni dopant form the Hirshfeld analysis but also verifies the strong orbital interaction and binding force in the new-formed bonds which contributes to such negative E_b.

The band structure (BS) of the pristine and Ni-decorated ZnO monolayer as well as the atomic density of state (DOS) of the new-bonded atoms in the Ni–ZnO systems are exhibited in Figure 2 to understand the electronic property of the ZnO monolayer through Ni-decorating. For the BS of the pristine ZnO monolayer, it is seen that its bandgap is obtained as 1.867 eV, agreeing with the previous report using the PBE function [34]. In terms of the Ni–ZnO monolayer, the bandgap in the current work is obtained as 0.896 eV, decreased by 0.971 eV compared with the pristine counterpart (that is, the Ni dopant induces a few novel states within the bandgap of the ZnO system, therefore narrowing its bandgap [18], which would be beneficial to enhance the chemical reactivity and electron

mobility of the whole system). From the atomic DOS of Ni, O and Zn atoms, one can see that the Ni 3*d* orbital is highly overlapped with the O 2*p* orbital around the Fermi level and is somewhat overlapped with the Zn 3*d* orbital at the state deep in the conduction band. In other words, the Ni dopant has much stronger orbital interaction with the O atom compared with the Zn atom. Overall, the Ni dopant conducts desirable binding force with the ZnO surface through decorating at the T_O site, which gives rise to the good chemical stability of the Ni–ZnO monolayer.
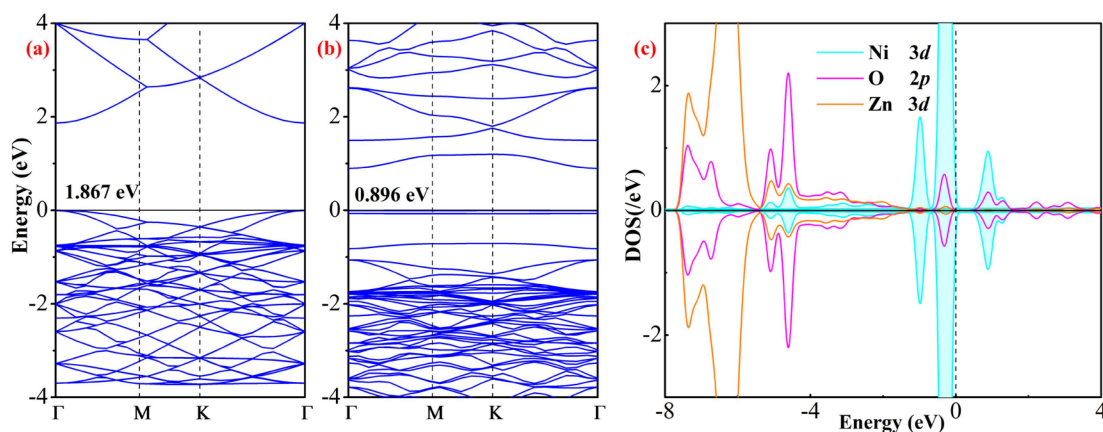

Figure 2. BS of (**a**) pristine ZnO monolayer (**b**) Ni–ZnO monolayer, and (**c**) atomic DOS of new-bonded atoms. In BS, the black value is the bandgap while in DOS the dash line is the Fermi level.

3.2. Analysis of Gas Adsorptions

The adsorption performance of the Ni–ZnO monolayer upon CO and HCHO molecule would be analyzed in this section. We first establish the adsorption configurations for two systems, in which the gas species are putting close to the Ni atom various morphologies for appropriate 2.5 Å to conduct the geometric optimizations. We define the adsorption energy (E_{ad1}) to help comprehend the binding performance of the Ni–ZnO monolayer upon the gas molecules, calculated by [35]:

$$E_{ad1} = E_{Ni-ZnO/gas} - E_{Ni-ZnO} - E_{gas} \qquad (2)$$

wherein $E_{Pd-ZnO/gas}$, E_{Pd-ZnO}, and E_{gas} indicate the energies of the Ni–ZnO/gas systems, isolated Ni–ZnO monolayer and gas molecule, respectively. With full relaxations, the most stable configuration (MSC) with the largest absolute value of E_{ad} can be determined, which would be analyzed in terms of their geometric and electronic properties. Besides, the adsorptions of CO and HCHO on the pristine ZnO monolayer are conducted in this work as well, and the adsorption configurations as well as their band structures are depicted in Figure S1 with corresponding analyses. The analyses show that the adsorption performance of the Ni–ZnO monolayer is dramatically stronger than the pristine ZnO monolayer. Therefore in the main body we focus on the Ni–ZnO/gas systems and to explore the sensing mechanism of the Ni–ZnO monolayer for gas detections.

Figure 3 plots the MSC and related CDD of the gas adsorbed systems. In the CO system, it can be seen that the CO molecule is somewhat parallel, keeping a small slope with the ZnO monolayer. The C and O atoms are both captured by the Ni dopant, forming the Ni–C and Ni–O bonds with bond lengths of 1.87 and 1.97 Å, respectively. In the meantime, the C–O bond length of the CO molecule is prolonged to 1.20 Å from that of 1.14 Å in its gas phase while the Ni–O and Ni–Zn bond lengths of the Ni–ZnO monolayer are prolonged to 1.83 and 2.66 Å from those of 1.80 and 2.54 Å in its isolated structure. These bond deformations indicate the geometric activations of the Ni–ZnO surface and the adsorbed CO molecule in the gas interactions [36]. Combined with the formed new bonds between them, one can assume that Ni–ZnO monolayer has desirable adsorption performance upon CO molecule. Such an assumption can be verified by the calculated E_{ad}

(-1.49 eV) in this system, whose absolute value is much larger than the critical value of 0.8 eV [37] to identify a chemisorption for this system. Based on the Hirshfeld analysis, the CO molecule is charged by -0.096 e and the Ni dopant is charged by 0.045 e. These findings indicate the electron-accepting property of the CO molecule and the Ni dopant in this system that withdraw 0.096 and 0.035 e, respectively. On the other hand, the ZnO surface behaves as an electron-donator releasing 0.131 e in the CO adsorption. These charge-transfer can cause the electron redistribution in the CO adsorbed system, deforming the electronic property of the Ni–ZnO monolayer accordingly [38]. From the CDD, the C–O bond of the CO molecule is surrounded by the electron depletion while the new-formed Ni–C and Ni–O bonds are surrounded by the electron accumulation, which manifests the weakness of the C–O bond accounting for its prolongation and the strong binding force of the Ni–C and Ni–O bonds accounting for their formations [39].
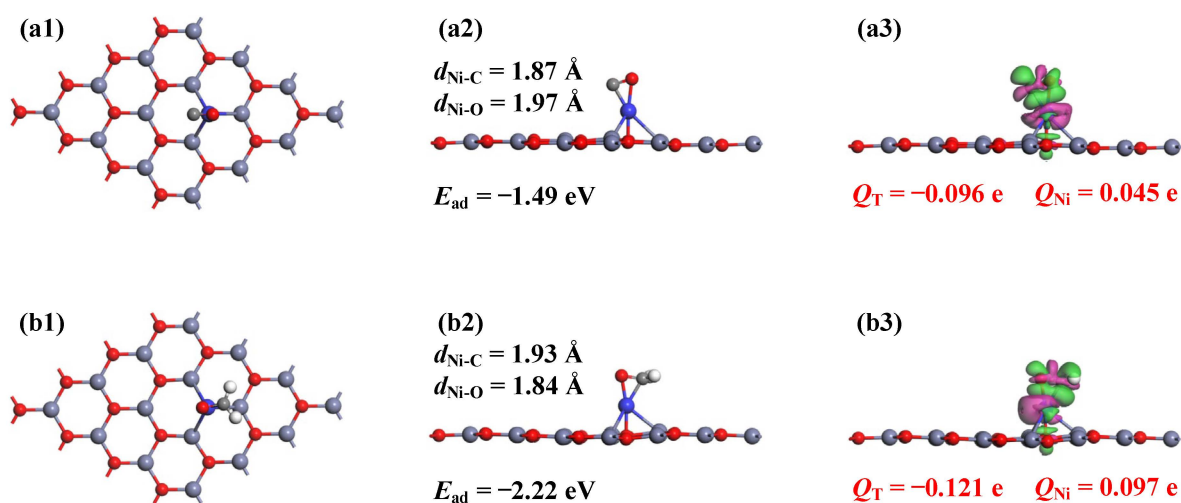

(a1)

(a2)
$d_{\text{Ni-C}} = 1.87$ Å
$d_{\text{Ni-O}} = 1.97$ Å

$E_{\text{ad}} = -1.49$ eV

(a3)
$Q_{\text{T}} = -0.096$ e $Q_{\text{Ni}} = 0.045$ e

(b1)

(b2)
$d_{\text{Ni-C}} = 1.93$ Å
$d_{\text{Ni-O}} = 1.84$ Å

$E_{\text{ad}} = -2.22$ eV

(b3)
$Q_{\text{T}} = -0.121$ e $Q_{\text{Ni}} = 0.097$ e

Figure 3. MSC and CDD of (**a1**–**a3**) HCHO system and (**b1**–**b3**) C_2H_3Cl system. In the CDD, the definitions are the same as Figure 1.

In terms of the HCHO system, the adsorption configuration is somewhat similar with that of the CO system. One can see that the HCHO molecule is basically parallel with the ZnO surface and the C and O atoms are trapped by the Ni dopant as well, with the formed Ni–C and Ni–O bonds measured to be 1.93 and 1.84 Å, respectively. It is worth noting that the Ni–C and Ni–O bond lengths in two systems are just reversed. Specifically, the Ni–C bond in the HCHO system is longer than that in the CO system while the length of the Ni–O bond in CO system is longer than that in the HCHO system. These may be attributed to the stronger chemical activity of the O atom in the HCHO molecule than that in the CO molecule [40], thus leading to the nearer atomic distance in the HCHO system. At the same time, the Ni–O and Ni–Zn bonds of the Ni–ZnO system are elongated to 1.84 and 2.64 Å, respectively, in comparison with those of 1.80 and 2.54 Å in the isolated Ni–ZnO monolayer. The E_{ad} in the HCHO system is calculated to be -2.22 eV, much more negative than that of the CO system implying the stronger interaction between Ni–ZnO monolayer and HCHO molecule. Also, the chemisorption can be determined as well here. From the Hirshfeld analysis, the HCHO molecule and Ni dopant are charged by -0.121 and 0.097 e, respectively. In comparison with the charged value of Ni dopant (0.080 e) in the isolated Ni–ZnO monolayer, one can deduce that the Ni dopant loses 0.017 e while the ZnO monolayer loses 0.104 e in the HCHO adsorption, which are all accepts by the HCHO molecule indicating its strong electron-accepting property. From the CDD, it is seen that the C–O and C–H bonds of the HCHO molecule are embraced by the electron depletion while the new-formed Ni–C and Ni–O bonds are embraced by the electron accumulations. Such phenomena are similar to that in the CO system confirming the weakened binding

force inside the HCHO molecule and the strong binding force between the Ni dopant and the HCHO molecule.

From the above analysis, one can find that the Ni–ZnO monolayer possesses desirably strong interactions with the CO and HCHO molecules, especially upon HCHO since in its adsorbed system the $|E_{ad}|$ and $|Q_T|$ are both larger than that in the CO system. Therefore, we presume that the deformation in the electronic property of the Ni–ZnO monolayer would be much more obvious in the HCHO system, thereby causing stronger sensing response for its detection. These analysis would be covered in the following sections. In the meanwhile, we find that compared with the previous report of Cu-decorated ZnO (Cu–ZnO) monolayer by Ma et al. [2], Ni–ZnO monolayer conducts weaker performance upon CO adsorption than Cu–ZnO monolayer with E_{ad} of −2.04 eV, but stronger performance than Cu–ZnO/HCHO system in which the E_{ad} is calculated as −1.66 eV.

3.3. Electronic Property Analysis

In order to comprehend electronic property of the Ni–ZnO monolayer upon gas adsorptions, Figure 4 exhibits the BS and atomic DOS of the CO and HCHO systems. From the BS of two gas adsorbed systems, one can see that their bandgaps are obtained as 1.155 and 0.800 eV, respectively. That is, the bandgap of the Ni–ZnO monolayer is increased by 0.259 eV (28.9%) in the CO system and decreased by 0.096 e V (10.7%) in the HCHO system. Such remarkable change of E_g could lead to significant change in the electrical resistance of the Ni–ZnO monolayer, thereby causing large enough sensing response for detection [41]. From this aspect, one can assume that Ni–ZnO monolayer can be explored as a promising sensing candidate for gas detection based on the change of electrical resistance. Detailed calculations about the sensing response can be found as follows.
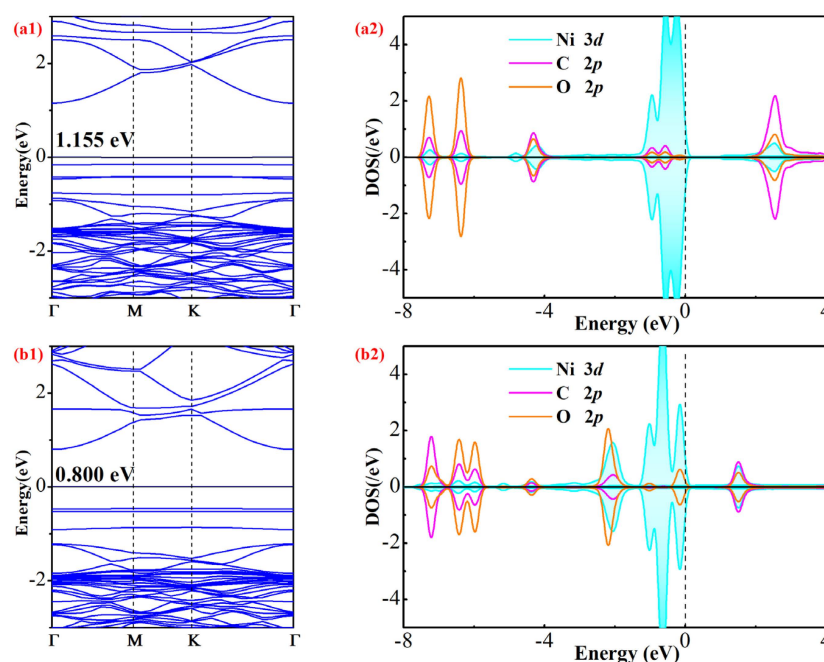

Figure 4. BS and atomic DOS of (**a1**,**a2**) CO system and (**b1**,**b2**) HCHO system. In BS, the black value is the bandgap while in DOS the Fermi level is set as 0.

From the atomic DOS of bonded atoms in CO system, it can be seen that the Ni 3*d* orbital is highly overlapped with the C 2*p* orbital around the Fermi level (−4.3, −0.9, −0.6 and 2.5 eV) while is overlapped with the O 2*p* orbital at the areas deep in the valence band (−7.3 and −6.4 eV). At the same time, the Ni 3d orbital at the HCHO system is highly overlapped with the O 2*p* orbital at around −0.1, −1.0, −2.2 (which are close to the Fermi level) whereas it is overlapped with the C 2*p* orbital at −7.2 eV and 1.5 eV (which are far away from the Fermi level). Considering the fact that the states around the Fermi level can

exert much stronger impact on the electronic property of the surface than those deep at the conduction band and valence band [42], one can presume that the orbital interaction of the Ni–C bond is much stronger than the Ni–O bond in the CO system while the Ni–O bond has stronger binding force than Ni–C bond in the HCHO system. These findings verify the above analysis about the binding force of Ni–C and Ni–O bonds in two systems from the aspect of bond lengths.

The work function (WF) is another parameter which reveals the material's performance to liberate an electron from its surface [43], which has a great influence on the surface dipole, charge transfer, and orbital localization of gas adsorption systems [44]. In this work, the WF of the pure Ni–ZnO system and the Ni–ZnO/gas systems are presented in Figure 5. It is found that the WF of the pure Ni–ZnO monolayer is obtained to be 4.35 eV, while those for the CO and HCHO systems are increased to be 4.84 and 4.46 eV, respectively. In other words, the WF of the Ni–ZnO monolayer undergoes pronounced increase by 0.49 eV (11.3%) and 0.11 eV (2.5%) after adsorptions of CO and HCHO molecule, and the change of WF in the CO system is great larger than the HCHO system, in agreement with the larger change of E_g in the former system. Therefore, we can infer that the Ni–ZnO monolayer can conduct much stronger sensitivity upon CO detection than HCHO based on the change of WF.
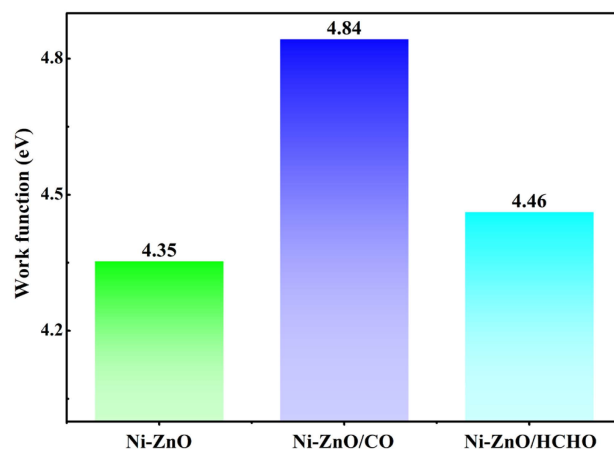

Figure 5. WF of pure Ni–ZnO monolayer and Ni–ZnO/gas systems.

3.4. Gas Sensor Explorations

It is concluded that the bandgap and WF of the Ni–ZnO monolayer are dramatically modulated after gas adsorptions, which provides the possibility for its exploration as a chemical gas sensor based on resistance or WF change in terms of CO or HCHO detection.

We first focus on the exploration of resistance-type gas sensor. As reported, the sensing response (S) of a resistance-type gas sensor is calculated by Equation (3) [45], wherein the electrical resistance (σ) of the sensing material can be calculated by Equation (4) which reveals its dependence with the bandgap (B_g). Besides, in Equation (4), the λ is a constant, k is the Boltzmann constant, and T is the temperature.

$$S = (\sigma_{gas}^{-1} - \sigma_{pure}^{-1})/\sigma_{pure}^{-1} \tag{3}$$

$$\sigma = \lambda \cdot e^{(-B_g/2kT)} \tag{4}$$

Using Equations (3) and (4), it is calculated that the sensing response of Ni–ZnO monolayer upon CO or HCHO detection is 15,394.9% and −84.6%, respectively. These findings manifest the desirable sensing responses of the Ni–ZnO monolayer in the CO or HCHO environment, especially for CO. Besides, these amounts of electrical responses, according to the previous report, can be feasibly detected by a electrochemical workstation [46]. In this respect, we presume that Ni–ZnO monolayer has strong potential to be applied as a resistance-type gas sensor in the electrical substation to detect CO or HCHO and to

reflect the working operation of the dry-type transformers. Moreover, the selectivity can be realized using the Ni–ZnO monolayer for detection of CO and HCHO in the single gas environment, especially for CO gas giving a much larger electrical response in the CO system.

Also, the recovery time (τ) should be considered as well to show the reusability of Ni–ZnO monolayer for gas detections, which is calculated by the van't-Hoff-Arrhenius expression [47] as displayed in Equation (5):

$$\tau = A^{-1}e^{(-E_{ad}/K_BT)} \tag{5}$$

wherein A is the attempt frequency (10^{12} s^{-1} [48,49]), T is temperature, and K_B is the Boltzmann constant (8.318×10^{-3} kJ/(mol·K)). One unfortunate thing is that the recovery time of the Ni–ZnO monolayer to desorb CO or HCHO molecule from its surface are 1.55×10^{13} and 3.39×10^{25} s, respectively, at room temperature (298 K). Although the improvement of the temperature can sharply decrease the recovery time, those for the CO and HCHO systems at 498 K are obtained as 1.18×10^3 and 2.87×10^{10} s, respectively. On the one hand, the recovery time can guarantee good interactions for the gas species staying on the Ni–ZnO surface to gain the good sensitivity for their detections [50,51]. On the other hand, such extremely long recovery time cannot make it realistic to reuse the sensor for gas detections. In other words, the Ni–ZnO monolayer can only be applied as a one-shot gas sensor for CO or HCHO detection with high sensitivity. Even considering the admirable sensing response of the Ni–ZnO monolayer upon CO or HCHO detection, we deem that the Ni–ZnO monolayer is a workable sensing material to evaluate the operation condition of the dry-type transformers through typical gas analysis.

Furthermore, according to the apparent changes of WF in the Ni–ZnO/gas systems in comparison to the isolated Ni–ZnO system, one can assume that the Ni–ZnO monolayer can also be applied in the Kelvin Probe system that works at WF detection [52] to reflect the existence of the CO or HCHO in the environment. In this regard, the sensitivity for CO detection is also higher than that of HCHO, due to the much higher WF in the CO system than HCHO system. Therefore, the selective detection of two such gases can also be realized, which provides another approach to evaluate the operation condition of the dry-type transformers.

4. Conclusions

In this work, the Ni–ZnO monolayer is proposed based on the first-principles calculations to study its sensing potential upon CO and HCHO in order to evaluate the operation condition of the dry-type transformers. The main conclusions are as follows:

(i) The T_O site is identified as the most preferred site for Ni-decorating on the pristine ZnO surface, with the E_b of -1.75 eV;

(ii) Chemisorption is determined for CO and HCHO systems given the admirable E_{ad} of -1.49 and -2.22 eV for their adsorption on the Ni–ZnO surface;

(iii) BS and WF analysis reveal the potential of Ni–ZnO monolayer as a resistance-type or Kelvin Probe gas sensor for CO and HCHO detection with high sensitivity and selectivity.

The findings of our theoretical calculations shed light on the ZnO-based gas sensor for application in the dry-type transformers, which can pave the way for toxic gas detections in many other fields.

Author Contributions: Conceptualization, J.Z. and T.Y.; Formal analysis, Z.W. and Q.W.; Writing—original draft preparation, Y.W. and Z.W.; Writing—review & editing, J.Z.; Funding acquisition, Z.L. and T.Y. All authors have read and agreed to the published version of the manuscript.

Conflicts of Interest: The authors declare no conflict of interest.

References

1. Yuan, T.; Fu, C.; Gong, Y.; Tong, Y.; Zhang, J.; Wang, Y. First-principles Insights into Cu-Decorated GaN Monolayers for Sensing CO and HCHO in Dry-Type Transformers. *ACS Omega* **2021**, *6*, 19127–19133. [CrossRef] [PubMed]
2. Pan, Z.; Wang, J.; Si, Q.; Shi, T.; Ma, S. Cu-decorated ZnO monolayer as a promising gas sensor in dry-type transformers: A first-principles study. *Comput. Theor. Chem.* **2021**, *1204*, 113429. [CrossRef]
3. Li, Y.; Guan, Y.J.; Li, T.Y. Calculation of Thermal Performance in Amorphous Core Dry-Type Transformers. *Adv. Mater. Res.* **2014**, *986–987*, 1771–1774. [CrossRef]
4. Xiong, L.; Zhao, Y.; Yang, Z.; Song, D.; He, W. Temperature rise analysis and calculation of cast resin dry-type transformers. *Gaodianya Jishu/High Volt. Eng.* **2013**, *39*, 265–271.
5. Wang, Y.; Feng, C.; Fei, R.; Luo, Y. Thermal-ageing characteristics of dry-type transformer epoxy composite insulation. *High Perform. Polym.* **2020**, *32*, 095400832090643. [CrossRef]
6. Zhang, Y.L.; Wang, L.; Xiong, L.; Zhao, Y.L.; Yang, Z.K.; Wei, H.E. On-line Temperature Monitoring and State Evaluation System for 10 kV Dry-type Transformers. *Electr. Meas. Instrum.* **2012**, *49*, 33.
7. Park, C.Y.; Park, D.W.; Choi, J.S.; Kil, G.S. A Study on PD Detection Methods for Cast-resin Dry-type Transformers. *J. Korean Inst. Electr. Electron. Mater. Eng.* **2009**, *22*, 786–791.
8. Patel, K.; Roondhe, B.; Dabhi, S.D.; Jha, P.K. A new flatland buddy as toxic gas scavenger: A first principles study. *J. Hazard. Mater.* **2018**, *351*, 337–345. [CrossRef]
9. Cui, H.; Kai, Z.; Zhang, Y.; Ye, H.; Chen, X. Superior Selectivity and Sensitivity of C_3N Sensor in Probing Toxic Gases NO_2 and SO_2. *IEEE Electron. Device Lett.* **2018**, *39*, 284–287. [CrossRef]
10. Cui, H.; Zhang, G.; Zhang, X.; Tang, J. Rh-doped $MoSe_2$ as toxic gas scavenger: A first-principles study. *Nanoscale Adv.* **2019**, *2019*, 772–780. [CrossRef]
11. Bradley, D. Graphene gas sensor. *Mater. Today* **2012**, *15*, 233. [CrossRef]
12. Chatterjee, S.G.; Chatterjee, S.; Ray, A.K.; Chakraborty, A.K. Graphene–metal oxide nanohybrids for toxic gas sensor: A review. *Sens. Actuators B Chem.* **2015**, *221*, 1170–1181. [CrossRef]
13. Xiaoxing, Z.; Lei, Y.; Xiaoqing, W.; Weihua, H. Experimental Sensing and Density Functional Theory Study of H_2S and SOF_2 Adsorption on Au-Modified Graphene. *Adv. Sci.* **2015**, *2*, 612.
14. Cui, H.; Jia, P.; Peng, X.; Hu, X. Geometric, Electronic and Optical Properties of Pt-Doped C_3N Monolayer Upon NOx Adsorption: A DFT Study. *IEEE Sens. J.* **2021**, *21*, 3602–3608. [CrossRef]
15. Luo, L.; Sosnowchik, B.D.; Lin, L. Local vapor transport synthesis of zinc oxide nanowires for ultraviolet-enhanced gas sensing. *Nanotechnology* **2010**, *21*, 495502. [CrossRef] [PubMed]
16. Chen, L.; Xiong, Z.; Cui, Y.; Luo, H.; Gao, Y. Adsorption of C_6H_6 and C_7H_8 onto pristine and metal (Pd, Pt)-mediated ZnO monolayers: Electronic and gas sensing properties. *Appl. Surf. Sci.* **2021**, *542*, 148767. [CrossRef]
17. Zhang, Y.-H.; Yue, L.-J.; Gong, F.-L.; Li, F.; Zhang, H.-L.; Chen, J.-L.J.V. Highly enhanced H_2S gas sensing and magnetic performances of metal doped hexagonal ZnO monolayer. *Vacuum* **2017**, *141*, 109–115. [CrossRef]
18. Qu, Y.; Ding, J.; Fu, H.; Peng, J.; Chen, H.J.A.S.S. Adsorption of CO, NO, and NH_3 on ZnO monolayer decorated with noble metal (Ag, Au). *Appl. Surf. Sci.* **2020**, *508*, 145202. [CrossRef]
19. Cao, W.; Zhao, Q.; Yang, L.; Cui, H. Enhanced NOx adsorption and sensing properties of $MoTe_2$ monolayer by Ni-doping: A first-principles study. *Surf. Interfaces* **2021**, *26*, 101372. [CrossRef]
20. Cui, H.; Zhang, X.; Li, Y.; Chen, D.; Zhang, Y. First-principles insight into Ni-doped InN monolayer as a noxious gases scavenger. *Appl. Surf. Sci.* **2019**, *494*, 859–866. [CrossRef]
21. Ma, Z.; Ren, F.; Deng, Y.; Volinsky, A.A.J.O. Structural, electrochemical and optical properties of Ni doped ZnO: Experimental and theoretical investigation. *Optik* **2020**, *219*, 165204. [CrossRef]
22. Wu, L.; Hou, T.; Wang, Y.; Zhao, Y.; Guo, Z.; Li, Y.; Lee, S.-T. First-principles study of doping effect on the phase transition of zinc oxide with transition metal doped. *J. Alloy. Compd.* **2012**, *541*, 250–255. [CrossRef]
23. Wang, X.; Zhao, M.; Liu, F.; Jia, J.; Li, X.; Cao, L. C_2H_2 gas sensor based on Ni-doped ZnO electrospun nanofibers. *Ceram. Int.* **2013**, *39*, 2883–2887. [CrossRef]
24. Li, P.; Hong, Q.; Wu, T.; Cui, H. SOF_2 sensing by Rh-doped PtS2 monolayer for early diagnosis of partial discharge in the SF_6 insulation device. *Mol. Phys.* **2021**, *119*, e1919774. [CrossRef]

25. Cui, H.; Liu, T.; Zhang, Y.; Zhang, X. Ru-InN Monolayer as a Gas Scavenger to Guard the Operation Status of SF6 Insulation Devices: A First-Principles Theory. *IEEE Sens. J.* **2019**, *19*, 5249–5255. [CrossRef]

26. Tkatchenko, A.; Jr, D.S.R.; Head-Gordon, M.; Scheffler, M. Dispersion-corrected Møller-Plesset second-order perturbation theory. *J. Chem. Phys.* **2009**, *131*, 171.

27. Chen, D.; Zhang, X.; Tang, J.; Cui, H.; Li, Y. Noble metal (Pt or Au)-doped monolayer MoS2 as a promising adsorbent and gas-sensing material to SO$_2$, SOF$_2$ and SO$_2$F$_2$: A DFT study. *Appl. Phys. A Mater. Sci. Process.* **2018**, *124*, 194. [CrossRef]

28. Cui, H.; Yan, C.; Jia, P.; Cao, W. Adsorption and sensing behaviors of SF6 decomposed species on Ni-doped C3N monolayer: A first-principles study. *Appl. Surf. Sci.* **2020**, *512*, 145759. [CrossRef]

29. Aretouli, K.E.; Tsipas, P.; Tsoutsou, D.; Marquez-Velasco, J.; Xenogiannopoulou, E.; Giamini, S.A.; Vassalou, E.; Kelaidis, N.; Dimoulas, A. Two-dimensional semiconductor HfSe2 and MoSe2/HfSe2 van der Waals heterostructures by molecular beam epitaxy. *Appl. Phys. Lett.* **2015**, *106*, 699. [CrossRef]

30. Ma, D.; Wang, Q.; Li, T.; Tang, Z.; Yang, G.; He, C.; Lu, Z. CO catalytic oxidation on Al-doped graphene-like ZnO monolayer sheets: A first-principles study. *J. Mater. Chem. C* **2015**, *3*, 9964–9972. [CrossRef]

31. Ma, D.; Ju, W.; Li, T.; Zhang, X.; He, C.; Ma, B.; Lu, Z.; Yang, Z. The adsorption of CO and NO on the MoS$_2$ monolayer doped with Au, Pt, Pd, or Ni: A first-principles study. *Appl. Surf. Sci.* **2016**, *383*, 98–105. [CrossRef]

32. Cui, H.; Jia, P.; Peng, X. Adsorption of SO$_2$ and NO$_2$ molecule on intrinsic and Pd-doped HfSe2 monolayer: A first-principles study. *Appl. Surf. Sci.* **2020**, *513*, 145863. [CrossRef]

33. Murphy, L.R.; Meek, T.L.; Allred, A.L.; Allen, L.C. Evaluation and test of pauling's electronegativity scale. *J. Phys. Chem. A* **2000**, *104*, 5867–5871. [CrossRef]

34. Peng, Q.; Liang, C.; Ji, W.; De, S. A first principles investigation of the mechanical properties of g-ZnO: The graphene-like hexagonal zinc oxide monolayer. *Comput. Mater. Sci.* **2013**, *68*, 320–324. [CrossRef]

35. Kou, L.; Frauenheim, T.; Chen, C. Phosphorene as a Superior Gas Sensor: Selective Adsorption and Distinct I–V Response. *J. Phys. Chem. Lett.* **2014**, *5*, 2675–2681. [CrossRef]

36. Fan, Y.; Zhang, J.; Qiu, Y.; Zhu, J.; Zhang, Y.; Hu, G. A DFT study of transition metal (Fe, Co, Ni, Cu, Ag, Au, Rh, Pd, Pt and Ir)-embedded monolayer MoS2 for gas adsorption. *Comput. Mater. Sci.* **2017**, *138*, 255–266. [CrossRef]

37. Han, S.W.; Cha, G.B.; Park, Y.; Hong, S.C. Hydrogen physisorption based on the dissociative hydrogen chemisorption at the sulphur vacancy of MoS$_2$ surface. *Sci. Rep.* **2017**, *7*, 7152. [CrossRef] [PubMed]

38. Ao, Z.M.; Yang, J.; Li, S.; Jiang, Q. Enhancement of CO detection in Al doped graphene. *Chem. Phys. Lett.* **2008**, *461*, 276–279. [CrossRef]

39. Ma, D.; Wang, Q.; Li, T.; He, C.; Ma, B.; Tang, Y.; Lu, Z.; Yang, Z. Repairing sulfur vacancies in the MoS$_2$ monolayer by using CO, NO and NO$_2$ molecules. *J. Mater. Chem. C* **2016**, *4*, 7093–7101. [CrossRef]

40. Lu, Z.; Yang, M.; Ma, D.; Lv, P.; Li, S.; Yang, Z.; Lu, Z.; Yang, M.; Ma, D.; Lv, P. CO oxidation on Mn-N4 porphyrin-like carbon nanotube: A DFT-D study. *Appl. Surf. Sci.* **2017**, *426*, 1232–1240. [CrossRef]

41. Chen, D.; Zhang, X.; Xiong, H.; Li, Y.; Tang, J.; Xiao, S.; Zhang, D. A First-Principles Study of the SF6 Decomposed Products Adsorbed Over Defective WS$_2$ Monolayer as Promising Gas Sensing Device. *IEEE Trans. Device Mater. Reliab.* **2019**, *19*, 473–483. [CrossRef]

42. A, X.H.; A, Y.G.; B, K.L.; A, L.X. Comparison of sensing and electronic properties of C2H2 on different transition metal oxide nanoparticles (Fe$_2$O$_3$, NiO, TiO$_2$) modified BNNT (10, 0). *Appl. Surf. Sci.* **2020**, *521*, 146463.

43. Cui, Z.; Wang, X.; Li, E.; Ding, Y.; Sun, C.; Sun, M. Alkali-metal-adsorbed g-GaN monolayer: Ultralow work functions and optical properties. *Nanoscale Res. Lett.* **2018**, *13*, 207. [CrossRef] [PubMed]

44. Li, F.; Gao, X.; Wang, R.; Zhang, T.; Lu, G.J.S.; Chemical, A.B. Study on TiO$_2$-SnO$_2$ core-shell heterostructure nanofibers with different work function and its application in gas sensor. *Sens. Actuators B Chem.* **2017**, *248*, 812–819. [CrossRef]

45. Verlag, S. Semiconductor Physical Electronics. *Semicond. Phys. Electron.* **2006**, *28*, 363–364.

46. Zhang, D.; Wu, Z.; Zong, X.; Zhang, Y. Fabrication of polypyrrole/Zn$_2$SnO$_4$ nanofilm for ultra-highly sensitive ammonia sensing application. *Sens. Actuators B Chem.* **2018**, *274*, 575–586. [CrossRef]

47. Zhang, Y.H.; Chen, Y.B.; Zhou, K.G.; Liu, C.H.; Zeng, J.; Zhang, H.L.; Peng, Y. Improving gas sensing properties of graphene by introducing dopants and defects: A first-principles study. *Nanotechnology* **2009**, *20*, 185504. [CrossRef]

48. Peng, S.; Cho, K.; Qi, P.; Dai, H. Ab initio study of CNT NO$_2$ gas sensor. *Chem. Phys. Lett.* **2004**, *387*, 271–276. [CrossRef]

49. Cui, H.; Chen, D.; Zhang, Y.; Zhang, X. Dissolved gas analysis in transformer oil using Pd catalyst decorated MoSe2 monolayer: A first-principles theory. *Sustain. Mater. Technol.* **2019**, *20*, e00094. [CrossRef]

50. Feng, Z.; Xie, Y.; Chen, J.; Yu, Y.; Zheng, S.; Zhang, R.; Li, Q.; Chen, X.; Sun, C.; Zhang, H. Highly sensitive MoTe$_2$ chemical sensor with fast recovery rate through gate biasing. *2D Mater.* **2017**, *4*, 025018. [CrossRef]

51. Cui, H.; Zhang, X.; Zhang, J.; Zhang, Y. Nanomaterials-based gas sensors of SF6 decomposed species for evaluating the operation status of high-voltage insulation devices. *High Volt.* **2019**, *4*, 242–258. [CrossRef]

52. Qazi, M.; Koley, G.; Park, S.; Vogt, T. NO$_2$ detection by adsorption induced work function changes in In$_2$O$_3$ thin films. *Appl. Phys. Lett.* **2007**, *91*, 043113. [CrossRef]